

# Siloxane Polymers Containing Azo Moieties Synthesized by Click Chemistry for Photo Responsive and Liquid Crystalline Applications

Someshwarnath Pandey, Balakrishna Kolli, Sarada P. Mishra, Asit B. Samui

Naval Materials Research Laboratory, Polymer Science and Technology Centre, Ambarnath-421506, India

Correspondence to: A. B. Samui (E-mail: absamui@gmail.com)

Received 2 November 2011; accepted 29 November 2011; published online 29 December 2011

DOI: 10.1002/pola.25885

**ABSTRACT:** Three new types of siloxane-based photoactive liquid crystalline polymers containing azo side groups were synthesized through the click chemistry route. The polymers having molecular weight range of 14,000–34,000 g mol<sup>-1</sup> were soluble in most of the polar solvents like chloroform, tetrahydrofuran, dimethylformamide, dimethyl sulfoxide, and dichloromethane. The photoresponsive *trans*–*cis* photoisomerization under UV radiation and *cis*–*trans* relaxation process in dark for the polymers were studied. The isomerization rate constants were found to be 0.01–0.04 sec<sup>-1</sup> and 1.16\*10<sup>-4</sup>–4.67\*10<sup>-4</sup> sec<sup>-1</sup>, respectively. It has been noted that the polymers showed high intensity absorption for n- $\pi^*$  in chloroform. Both *trans* and *cis* forms of azide monomers having azo moiety exhibited molar extinction coefficient ( $\epsilon_{\max}$ ) in the range of

22,000–33,000 L mol<sup>-1</sup> cm<sup>-1</sup>. The thermotropic behavior of the polymers was studied by polarizing optical microscope (POM) and differential scanning calorimetry (DSC) experiments. Polymer P1 showed liquid crystalline textures of nematic droplets, whereas P2 showed smectic focal conic texture and nematic droplets. Polymer P1 was also studied for photomechanical bending on exposure to UV radiation. The polymers showed initial degradation temperature in the range of 210–275°C. © 2011 Wiley Periodicals, Inc. *J Polym Sci Part A: Polym Chem* 50: 1205–1215, 2012

**KEYWORDS:** azo polymers; click chemistry; differential scanning calorimetry (DSC); liquid crystalline; nematic; photoswitching; polysiloxanes; smectic; UV–vis spectroscopy

**INTRODUCTION** Azo polymers are well known for their *trans*–*cis* isomerization. The two isomers can switch between them with specific irradiations.<sup>1</sup> The photo-isomerization of azobenzene is also designated by a form of light-induced molecular motion.<sup>2–4</sup> Further as research has progressed, more and more applications started emerging such as, photo-switching, information storage, holography, etc.<sup>5</sup> The azo polymers are also found to have LC properties due to the rod-like nature of azo benzene moiety.<sup>6</sup> The basic properties of side-chain liquid crystal polymers have been extensively studied because of their potential applications in nonlinear optics, information storage, and display devices, etc.<sup>7</sup>

Molecular engineering of side chain liquid crystalline polymer, by living cationic polymerization, was published by Percec et al.<sup>8</sup> Flexible backbone was selected to tailor the LC transition temperatures. Side chain branched polymers were beginning to show their usefulness in a big way due to their property of self assembly which made them eligible for showing excellent optical properties.<sup>9</sup> Percec et al. investigated the changes in structure with temperature for the supramolecular structure formed by a poly(methacrylate) with tapered side chains.<sup>10</sup> Cylindrical and spherical assembly was developed further by starting with amphiphilic den-

drons.<sup>11</sup> Stabilization of a hexagonal columnar mesophase, generated from supramolecular and macromolecular columns, was also reported.<sup>12</sup> Isomerization of helical dendronized polyphenylacetylenes was reported in the series.<sup>13</sup> One interesting review article by the same author appeared very recently, which deals with the pattern of self organization in conventional functional polymers, where the functional group was replaced with a dendron.<sup>14</sup>

While the implication of structural parameters affecting the properties were given importance, a new area emerged, which was concerned with the application of various design so that it was very close to mimicking biological systems. A library of amphiphilic dendritic dipeptides that self-assemble in solution and in bulk through a complex recognition process into helical pores was described by Percec et al.<sup>15</sup> The molecular recognition and self-assembly process was found to be sufficiently robust to tolerate a series of modifications to the amphiphile structure. Attaching conducting organic donor or acceptor groups to the apex of a dendron leads to supramolecular nanometer-scale columns that contain  $\pi$ -stacks of donors, acceptors, or donor–acceptor complexes in their cores which imparted them high charge carrier mobilities.<sup>16</sup>

The synthesis and calorimetric properties of azo methacrylate was reported by Angeloni et al.<sup>17</sup> The strategy of synthesizing side chain liquid crystalline polymers depends mostly on methacrylates and siloxane having pendant LC molecules. The strategies adopted are very important as it affects the final shape and properties of the polymer. There are a number of reports that encompass a variety of synthetic strategies while considering chain conformation, association, degree of polymerization, and other related parameters.<sup>18–24</sup> The complexation of small molecules with salts can also impart specific properties to the associated species such as stabilization of the mesophase.<sup>25</sup> Molecular weight plays also a major role in exhibiting the LC nature of the polymers.<sup>26</sup>

The first report of both photoexpanded and photocontracted surface patterns in the same material, at different temperatures, was published by Yager et al.<sup>27</sup> Later it was identified as photomechanical effect. The photoisomerization of LC moieties to impart actuator effect in materials was first proposed by de Gennes et al.<sup>28</sup>

Thus, the theoretical aspects combined with potential uses in devices affected increasing interest in their synthesis for various applications.<sup>29</sup> A lot of work has been done to realize the above effects by designing mainly side chain liquid crystalline azo polymer. Encompassing all the efforts, these polymers have been the subject of intense study for quite a long time.<sup>30</sup> The proportion and positional role of the photosensitive groups in the crosslinked polymer network influence different types and magnitudes of responses.<sup>31</sup> Photoisomerization-induced phase transition of liquid-crystalline azobenzene chromophore and its influence on the phase diagrams of its mixtures with reactive mesogenic diacrylate monomer has also been investigated both theoretically and experimentally.<sup>32</sup>

Siloxane based side-chain azo polymers can be considered as a class of photoactive material due to the chain flexibility which will help in rapid photoactuation. Their other properties are easy processability, high thermoxidative stability, low surface energy, high chemical resistance, and good film forming properties, etc. In addition, as siloxane units are highly flexible, they are expected to show a lower liquid crystalline transition temperature as compared to the carbon analogues.<sup>33</sup> A great number of studies have been reported on liquid crystalline polymers incorporating siloxane as a flexible spacer in the main chain that includes polysiloxane liquid crystalline polymer, which was first synthesized by Finkelmann et al. through hydrosilylation reaction between hydrogen containing silicone-oil and vinyl liquid crystalline monomers.<sup>34</sup> Recently, Mather et al. have also reported the synthesis of main-chain siloxane-based liquid crystalline polymer for soft actuation devices.<sup>35</sup> A wide range of liquid crystalline polysiloxanes possessing half-disk and rod-like moieties,<sup>36</sup> methyl stilbene groups,<sup>37</sup> macroheterocyclic ligands,<sup>38</sup> have been reported. Percec et al. reported a microphase-separated morphology in siloxane-based LC polymer consisting of main chain and side chain domains.<sup>39,40</sup> Racles et al. reported the synthesis of siloxane-based liquid crystalline photoactive polyethers.<sup>41</sup> Therefore, siloxane-based poly-

meric liquid crystalline materials with azobenzene moieties could be promising materials for both optical switching and image storage as the orientation of mesogens in the thin films of these materials can be modified by light.

In this article we report the synthesis of various siloxane-based polymers, containing azo as pendent group, by using the click chemistry route. Although there are several reports in the literature regarding the synthesis of azo polymers by click chemistry, few of them suffered from solubility and processability problems.<sup>42</sup> In this work we have incorporated a siloxane unit in the main chain as a flexible spacer by the click chemistry route. The polymers were characterized by electronic spectroscopy, thermogravimetry, differential scanning calorimetry, and hot stage optical microscopy. The kinetic study on isomerization has also been studied.

## EXPERIMENTAL

### Materials

Propargyl bromide, 1,1,3,3,5,5-hexamethyl trisiloxane, 2% platinum(0)-1,3-divinyl-1,1,3,3-tetramethyl disiloxane complex in xylene (karstedt's catalyst), allyl alcohol, aniline, *n,n*-bis(diethanol)aniline, aniline, sodium-ascorbate, 4,4-dimethyl amino pyridine (DMAP), dicyclohexyl carbodimide (DCC), and phosphorus oxychloride (POCl<sub>3</sub>) were purchased from Sigma-Aldrich. All other chemicals were purchased from SD Fine Chemicals, India. All solvents were purchased from Merck India Pvt. Ltd. THF and toluene were dried over sodium-ketyl radical. All the chemicals were used as received without further purifications unless otherwise specified.

### Characterization

UV-Visible spectra of the polymers were taken on a Cary 500 Scan UV-Vis-NIR spectrophotometer. <sup>1</sup>H and <sup>13</sup>C NMR spectra of the monomers and the polymers were recorded on either a 500-MHz Bruker-FT NMR spectrometer or a 300-MHz JEOL-FT NMR spectrometer. Thermogravimetric analysis (TGA) was performed with a TA instruments His Res TGA 2950 with a heating rate of 20°C/min under N<sub>2</sub> atmosphere. Heating/cooling rate used for all DSC analysis was 10°C/min. For studying the liquid crystalline behavior, a Leica DMLD, an optical polarizing microscope with image analyzer equipped with LINKAM TMS 94 hot stage, and a LINKAM LNP controlling unit were used. The molar extinction coefficients (ε<sub>max</sub>) of diazide azo monomers were calculated by following the procedure described by Zhu et al.<sup>23</sup> For photoresponsive studies the samples were irradiated in the cabinet of a UV chamber (Spectrolinker XL – 1500) with 6 × 15 Watt medium pressure mercury bulbs. The sample was placed at a distance of 15 cm from the irradiation source for various time intervals.

### Methods

#### Synthesis of Methyl 4-(prop-2-ynyloxy) Benzoate (1)

Scheme 1 shows the synthesis of diyne and diazide monomers. To a solution of methyl 4-hydroxy benzoate (5 g, 33 mmol) in DMF (40 mL), K<sub>2</sub>CO<sub>3</sub> (16.67 g, 120 mmol) was added. The mixture was heated to 80°C for 30 min followed by dropwise addition of propargyl bromide (80% in toluene)

(7.4 mL, 50 mmol). The reaction mixture was stirred at the same temperature for additional 12 h, quenched in cold water, and extracted with chloroform. The organic layer was washed with water, dried over anhydrous Na<sub>2</sub>SO<sub>4</sub> and evaporated under vacuum. The product was purified by column chromatography using ethyl acetate and pet ether (5:95 v/v) to obtain off-white colored waxy solid.

Yield: 4.6 g (74.6%); <sup>1</sup>H NMR (500 MHz, CDCl<sub>3</sub>) δ: 2.54 (t, *J* = 2.5 Hz, 1H), 3.88 (s, 3H), 4.74 (d, *J* = 2.5 Hz, 2H), 6.99 (d, *J* = 8.5 Hz, 2H), 8.00 (d, *J* = 9.0 Hz, 2H); <sup>13</sup>C NMR (125 MHz, CDCl<sub>3</sub>) δ: 51.86, 55.78, 76.05, 77.79, 114.51, 123.42, 131.50, 161.11, 166.64.

#### 4-(Prop-2-ynyloxy) Benzoic Acid (2)

4-(prop-2-ynyloxy) benzoate (1) (3.5g, 18.4 mmol) was dissolved in a mixed solvent of tetrahydrofuran (THF) (20 mL) and methanol (10 mL). To the solution, an aqueous solution of sodium hydroxide (40%, 10 mL) was added. The reaction mixture was allowed to reflux for 2 h. The organic solvent was distilled off under vacuum and water was added to make a clear solution. The solution was acidified by addition of conc. HCl acid. The precipitate obtained was filtered, washed with water, and dried under vacuum to obtain a white solid.

Yield: 2.6 g (80.2 %); <sup>1</sup>H NMR (500 MHz, CDCl<sub>3</sub>) δ: 3.59 (s, 1H), 4.86 (d, *J* = 2.0 Hz, 2H), 7.04 (d, *J* = 9.0 Hz, 2H), 7.88 (d, *J* = 9.0 Hz, 2H); <sup>13</sup>C NMR (125 MHz, CDCl<sub>3</sub>) δ: 39.91, 56.05, 79.02, 79.14, 115.04, 124.11, 131.67, 161.13.

#### Trisiloxane-Diol (3)<sup>43</sup>

To a solution of allyl-alcohol (11.2 g, 193 mmol) in anhydrous toluene (25 mL), Karstedt's catalyst (0.45 mL) was added. It was followed by dropwise addition of 1, 1, 3, 3, 5, 5-hexamethyl trisiloxane (10 g, 48 mmol) over half an hour at 50°C. After the addition was complete, the temperature was raised to 70°C and the reaction continued up to 48 h. Progress of the reaction was monitored through disappearance of Si—H peak in IR spectra at 2163 cm<sup>-1</sup>. Toluene and excess allyl alcohol were removed by distillation. The crude product was dissolved in 30 mL dichloromethane (DCM) and purified by passing through a bed of alumina followed by evaporation of solvent under vacuum to yield a colorless viscous liquid.

Yield: 14.5 g, (93.1 %); <sup>1</sup>H NMR (300 MHz, CDCl<sub>3</sub>) δ: 0.01 (s, 18H), 0.50 (s, 4H), 1.52 (s, 4H), 2.60 (bs, 2H), 3.50 (s, 4H); <sup>13</sup>C NMR (125 MHz, CDCl<sub>3</sub>): 0.92, 1.87, 13.87, 26.38, 65.25.

#### Trisiloxane-Diyne (4)

4-(prop-2-ynyloxy) benzoic acid (2) (3g, 17.1 mmol), trisiloxane-diol (3) (2.3g, 7.1 mmol), DMAP (0.19 g, 1.5 mmol) and 25 mL of anhydrous THF were taken in a 100-mL round bottom flask. The flask was made air tight by using a rubber septum. Nitrogen gas was continuously passed through schlenk tube. A solution of DCC (3.07 g, 15 mmol) in 5 mL THF was added to the round bottom flask through the septum via a syringe. The mixture was allowed to stir under nitrogen for 48 h. The reaction mixture was filtered and the organic phase was evaporated. The residue was purified by column chromatography by using a mixture of petroleum

ether and ethyl acetate (98:2) eluant to obtain the product as colorless oil.

Yield: 3.5 g, (77 %); <sup>1</sup>H NMR (500 MHz, CDCl<sub>3</sub>) δ: 0.03 (s, 6H), 0.09 (s, 12H), 0.61 (t, *J* = 8.5 Hz, 4H), 1.76 (q, *J* = 7.0 Hz, 4H), 2.53 (t, *J* = 2.0 Hz, 2H), 4.23 (t, *J* = 6.5 Hz, 4H), 4.72 (d, *J* = 4.0 Hz, 4H), 6.98 (d, *J* = 9.0 Hz, 4H), 8.00 (d, *J* = 9.0 Hz, 4H); <sup>13</sup>C NMR (125 MHz, CDCl<sub>3</sub>) δ: 1.14, 1.24, 14.13, 22.74, 55.77, 67.13, 76.00, 77.83, 114.41, 123.81, 131.45, 161.04, 166.14

#### *N,N*-Bis-(2-chloroethyl)-aniline (5)

The synthesis was carried out by following the procedure as reported by Shen et al.<sup>44</sup> *N,N*-diethanol aniline was converted to *N,N*-dichlorodiethyl aniline using POCl<sub>3</sub> as chlorinating agent.

#### Synthesis of Azo Compound (6)

The synthesis of azo compound was carried out as reported by Shen et al.<sup>44</sup> In a typical recipe aniline (2 g, 21.5 mmol) was added to 40 mL of 5M HCl at 0°C. To the mixture, ice-cooled aqueous saturated solution of sodium nitrite (1.78 g, 25.8 mmol) was added maintaining the temperature between 0 and 5°C. This mixture was then added dropwise to another round bottom flask containing *N,N*-bis(2-chloroethyl)-aniline (5) (4.68 g, 21.5 mmol) dissolved in ethanol and maintained at 0°C (3% solution w/v). During addition, the temperature was not allowed to rise above 10°C. The stirring was continued for 4 h at the same temperature and then warmed to room temperature. The reaction mixture was filtered, washed several times with water, dried, and recrystallized from 2-methoxyethanol to obtain the product as a red solid.

Yield: 5.1 g, (71 %); <sup>1</sup>H NMR (500MHz, CDCl<sub>3</sub>) δ: 3.69 (t, *J* = 7.0 Hz, 4H), 3.84 (t, *J* = 7.0 Hz, 4H), 6.77 (d, *J* = 9.0 Hz, 2H), 7.39–7.42 (m, 1H), 7.47–7.50 (m, 2H), 7.85 (d, *J* = 7.5 Hz, 2H), 7.90 (d, *J* = 7.0 Hz, 2H); <sup>13</sup>C NMR (125 MHz, CDCl<sub>3</sub>) δ: 40.23, 53.46, 111.59, 122.35, 125.23, 128.97, 129.87, 144.64, 148.45, 152.97.

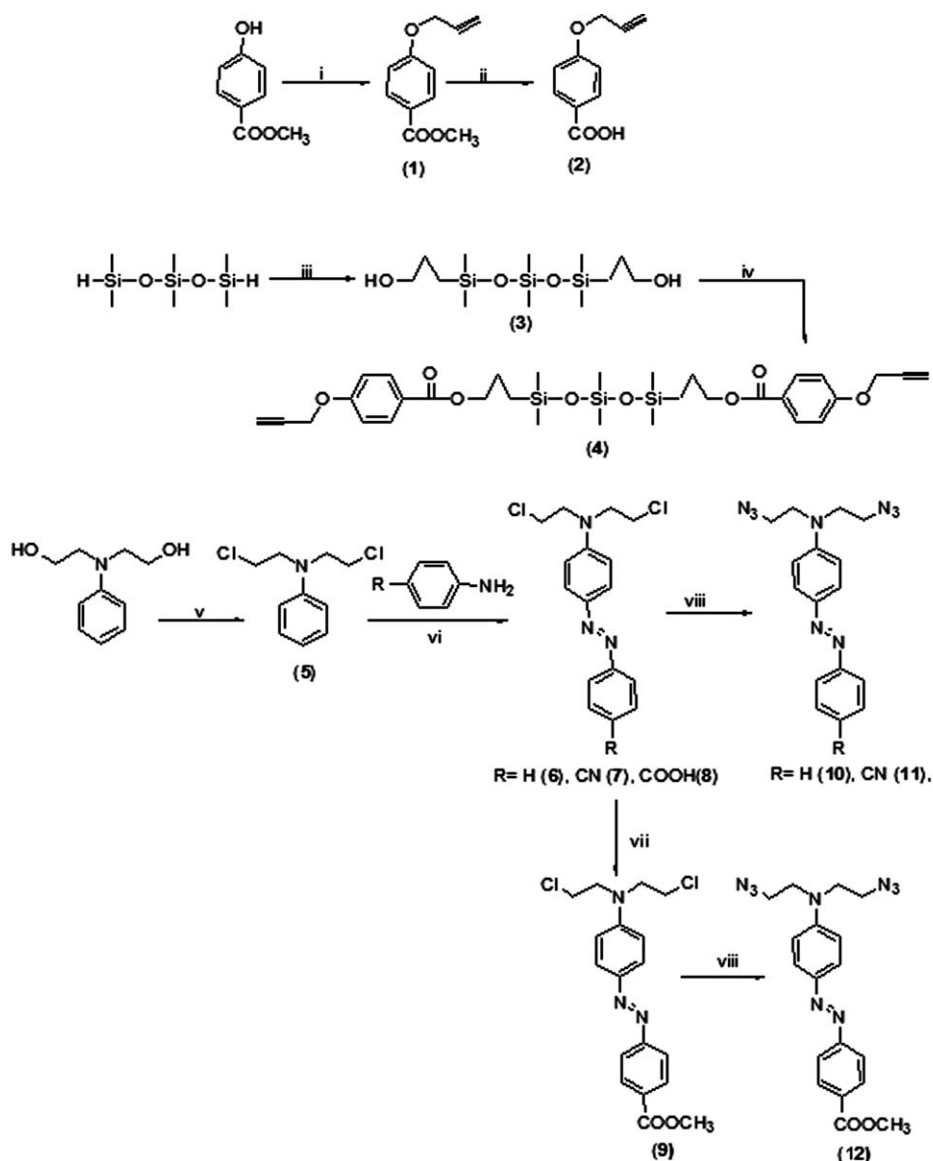
#### 4-((4-(Bis-(2-chloroethyl) amino) phenyl) diazenyl) Benzonitrile (7)

The synthesis was carried out by using same procedure as mentioned for product 6 except the use of aniline. In this case —CN (cyano) group was present at the para position and the product was recrystallized from a water-ethanol mixture.

Yield: 6.58 g, (85 %); <sup>1</sup>H NMR (500 MHz, CDCl<sub>3</sub>) δ : 3.71 (t, *J* = 6.5 Hz, 4H), 3.86 (t, *J* = 7.0 Hz, 4H), 6.78 (d, *J* = 9.0 Hz, 2H), 7.77 (d, *J* = 8.0 Hz, 2H), 7.91 (d, *J* = 8.0 Hz, 2H), 7.92 (d, *J* = 9.0 Hz, 2H); <sup>13</sup>C NMR (125 MHz, CDCl<sub>3</sub>) δ: 40.45, 53.75, 111.97, 112.81, 119.09, 123.17, 126.30, 133.39, 144.87, 149.85, 155.40.

#### 4-((4-Bis-(2-chloroethyl) amino) phenyl) diazenyl) Benzoic Acid (8)

The synthesis was carried out by using the same procedure as mentioned for product 6, except the use of aniline. Para-amino benzoic acid was used in this case and the product was recrystallized from a water-ethanol mixture.



**SCHEME 1** Synthesis of siloxane-diyne and diazide monomers.

Yield: 7.2 g (89%);  $^1H$  NMR (500 MHz,  $DMSO-d_6$ )  $\delta$ : 3.81 (t,  $J = 4.5$  Hz, 4H), 3.88 (t,  $J = 4.5$  Hz, 4H), 6.95 (d,  $J = 6.5$  Hz, 2H), 7.84–8.09 (m, 6H);  $^{13}C$  NMR (125 MHz,  $DMSO-d_6$ )  $\delta$ : 41.40, 52.36, 112.43, 122.30, 125.80, 130.93, 131.71, 143.91, 150.49, 155.35, 167.27.

#### Synthesis of Methyl 4-((4-Bis(2-chloroethyl) amino) phenyl) diazenyl) Benzoate (9)

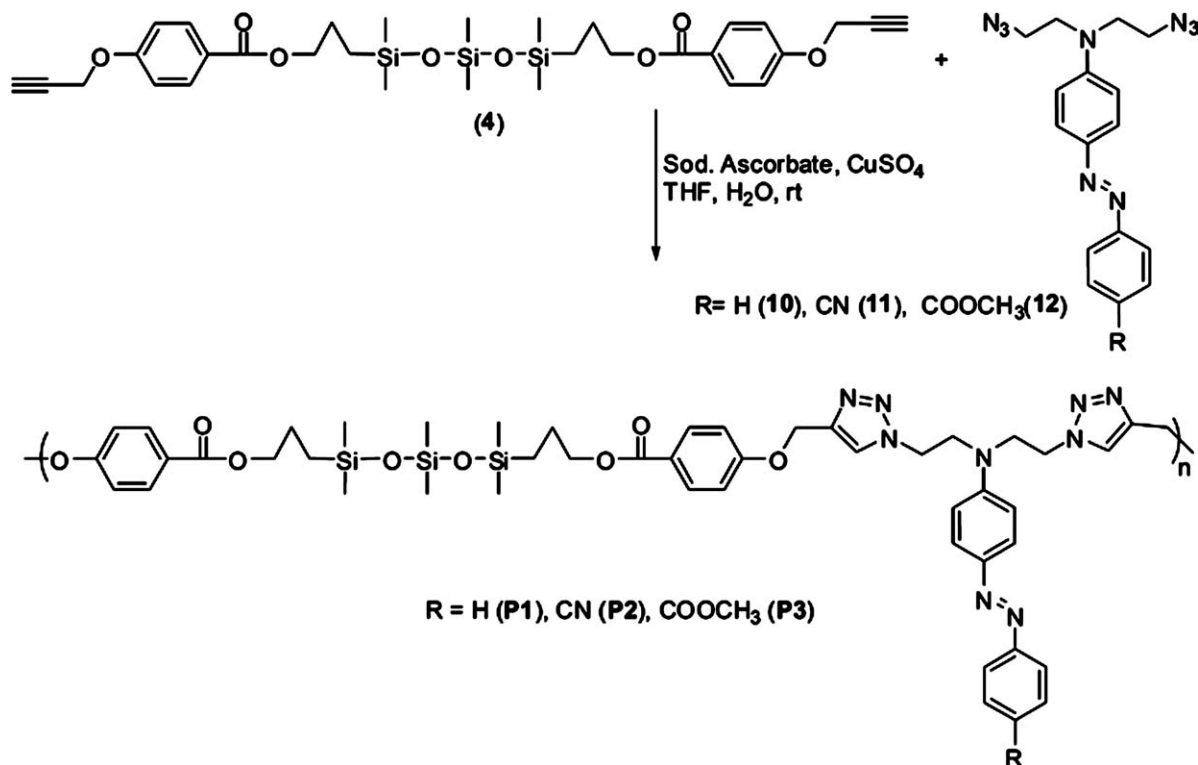
To a solution of 4-((4-bis(2-chloroethyl) amino) phenyl) diazenyl) benzoic acid (8) (2 g, 5.27 mmol) in methanol (100 mL), two drops of conc.  $H_2SO_4$  was added. The solution was refluxed for 24 h. The reaction mixture was cooled to room temperature and added to ice cold water. The product was extracted in chloroform, washed with saturated solution of  $NaHCO_3$ , dried over  $Na_2SO_4$ , and evaporated under vacuum.

The purification was done by column chromatography using a mixture of ethyl acetate and petroleum ether (20:80 v/v). An orange solid product was obtained.

Yield: 1.6 g (77 %);  $^1H$  NMR (500 MHz,  $CDCl_3$ )  $\delta$ : 3.70 (t,  $J = 7.0$  Hz, 4H), 3.85 (t,  $J = 6.5$  Hz, 4H), 3.94 (s, 3H), 6.78 (d,  $J = 9.0$  Hz, 2H), 7.87 (d,  $J = 8.5$  Hz, 2H), 7.92 (d,  $J = 8.5$  Hz, 2H), 8.15 (d,  $J = 8.0$  Hz, 2H);  $^{13}C$  NMR (125 MHz,  $CDCl_3$ )  $\delta$ : 40.17, 52.18, 53.44, 111.62, 122.14, 125.70, 130.52, 130.64, 144.67, 149.08, 155.64, 166.68.

#### Representative Example of Synthesis of Azo-Diazide (10)<sup>44</sup>

To a solution of *N,N*-bis(2-chloroethyl)-4-(phenyldiazenyl)aniline (6) (2 g, 6.2 mmol) in DMSO (10 mL), sodium azide



**SCHEME 2** Synthesis of azo containing siloxane polymers by click chemistry.

(1.1 g, 16.9 mmol) was added. The reaction mixture was heated at 90°C for 5 h and cooled to room temperature and poured into dilute HCl (5%, 15 mL). The compound was extracted with dichloromethane. The organic layer was washed with water, dried over Na<sub>2</sub>SO<sub>4</sub>, and evaporated under vacuum. Purification of the product was done by column chromatography using petroleum ether and ethyl acetate mixture (95:5; v/v).

Yield: 1.97 g, (95%); <sup>1</sup>H NMR (500 MHz, CDCl<sub>3</sub>) δ: 3.56 (t, *J* = 6.0 Hz, 4H), 3.69 (t, *J* = 6.0 Hz, 4H), 6.79 (d, *J* = 9.0 Hz, 2H), 7.39–7.50 (m, 3H), 7.47–7.50 (m, 2H), 7.85 (d, *J* = 8.0 Hz, 2H), 7.89 (d, *J* = 7.0 Hz, 2H); <sup>13</sup>C NMR (125 MHz, CDCl<sub>3</sub>) δ: 48.76, 50.77, 111.90, 122.33, 125.19, 128.98, 129.83, 144.58, 148.65, 153.01.

#### 4-((4-Bis(2-azidoethyl) amino) phenyl) diazenyl) Benzonitrile (11)

The synthesis was carried out by using (7) as starting material following the method as used for synthesis of (10).

Yield: 2.02 g, (91 %); <sup>1</sup>H NMR (500 MHz, CDCl<sub>3</sub>) δ: 3.59 (t, *J* = 6.0 Hz, 4H), 3.71 (t, *J* = 6.0 Hz, 4H), 6.82 (d, *J* = 3.0 Hz, 2H), 7.76 (d, *J* = 8.0 Hz, 2H), 7.90 (d, *J* = 8.5 Hz, 2H), 7.92 (d, *J* = 9.0 Hz, 2H); <sup>13</sup>C NMR (125 MHz, CDCl<sub>3</sub>) δ: 48.76, 50.74, 111.87, 112.35, 118.91, 122.83, 125.96, 133.07, 144.46, 149.69, 155.17.

#### Methyl 4-((4-Bis(2-azidoethyl) amino) phenyl) diazenyl) Benzoate (12)

The synthesis was carried out by using (9) as starting material following the method as used for the synthesis of (10).

Yield: 2.07 g, (85 %); <sup>1</sup>H NMR (500 MHz, CDCl<sub>3</sub>) δ: 3.58 (t, *J* = 6.0 Hz, 4H), 3.70 (t, *J* = 6.0 Hz, 4H), 3.94 (s, 3H), 6.80 (d, *J* = 9.0 Hz, 2H), 7.87 (d, *J* = 8.5 Hz, 2H), 7.92 (d, *J* = 9.0 Hz, 2H), 8.15 (d, *J* = 8.5 Hz, 2H); <sup>13</sup>C NMR (125 MHz, CDCl<sub>3</sub>) δ: 48.77, 50.75, 52.17, 111.86, 122.11, 125.67, 130.52, 130.58, 144.61, 149.27, 155.69, 166.70.

#### Synthesis of Polymers by Click-polymerization (P1)

Scheme 2 shows the synthesis of azo-siloxane polymer by click chemistry route.

A mixture of trisiloxane-diyne (4) (0.20 g, 0.312 mmol), *N,N*-bis(2-azidoethyl)-4-(phenyldiazenyl) aniline (9) (0.10 g, 0.312 mmol), and sodium ascorbate (0.130 g, 0.656 mmol) was taken in 3 mL of THF. The mixture was allowed to stir under nitrogen atmosphere for 10 min. A solution of copper sulfate (0.086 g, 0.34 mmol) in 3 mL of water was added to it. The reaction mixture was allowed to stir for additional 40 min under N<sub>2</sub> atmosphere and quenched with methanol (20 mL). The precipitate was filtered, dissolved in THF, and passed through an alumina bed to remove the catalyst and insoluble impurities. The THF solution was then evaporated to obtain the polymer (P1) as a red powder. Similarly, polymers P2 and P3 were synthesized by reacting (4) with (10) and (11), respectively.

Yield: 0.22 g, (73 %); <sup>1</sup>H NMR (500 MHz, CDCl<sub>3</sub>) δ: 0.06–0.08 (bs, 18H), 0.59 (bs, 4H), 1.24 (bs, 4H), 3.53–3.60 (bs, 4H), 4.20 (bs, 4H), 4.38 (bs, 4H), 5.17 (bs, 4H), 6.64–7.95 (bs, 17H), 7.46 (bs, 1H); <sup>13</sup>C (125 MHz, CDCl<sub>3</sub>) δ: 0.95, 1.23, 14.10, 22.71, 47.31, 51.46, 61.71, 67.19, 112.19, 114.35,

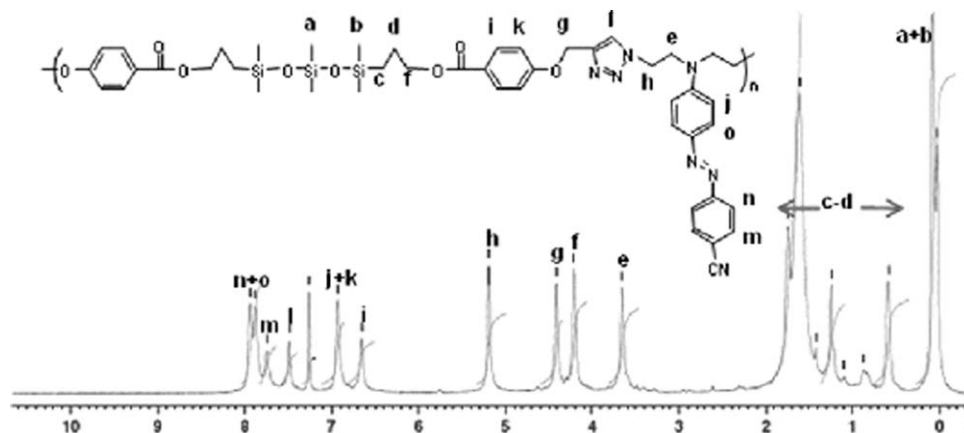


FIGURE 1  $^1\text{H}$  NMR spectra of polymer P2.

122.42, 123.95, 125.31, 129.00, 130.16, 131.52, 143.74, 145.06, 147.49, 152.80, 161.57, 166.14.

### P2

Yield: 0.22 g, (71.2 %);  $^1\text{H}$  NMR (500 MHz,  $\text{CDCl}_3$ )  $\delta$ : 0.02–0.09 (br, 18H), 0.59 (bs, 4H), 1.25 (bs, 4H), 3.65 (bs, 4H), 4.21 (bs, 4H), 4.41 (bs, 4H), 5.19 (bs, 4H), 6.65–7.90 (br, 16H), 7.25 (bs, 1H);  $^{13}\text{C}$  NMR (125 MHz,  $\text{CDCl}_3$ )  $\delta$ : 0.10, 1.25, 14.11, 22.73, 47.33, 51.40, 61.73, 67.22, 112.07, 114.37, 115.12, 118.68, 122.95, 126.06, 131.53, 133.10, 143.93, 144.86, 148.10, 154.30, 161.58, 166.15.

### P3

Yield: 0.25 g, (77 %);  $^1\text{H}$  NMR (500 MHz,  $\text{CDCl}_3$ )  $\delta$ : 0.02–0.09 (br, 18H), 0.59 (bs, 4H), 1.10 (bs, 4H), 3.64 (bs, 4H), 3.93 (bs, 3H), 4.21 (bs, 4H), 4.40 (bs, 4H), 5.18 (bs, 4H), 6.60–8.20 (br, 16H), 7.48 (bs, 2H);  $^{13}\text{C}$  NMR (300 MHz,  $\text{CDCl}_3$ )  $\delta$ : 0.10, 14.09, 22.71, 47.31, 51.41, 52.21, 61.71, 67.20, 112.08, 114.34, 122.21, 123.57, 123.97, 125.78, 130.54, 131.52, 143.82, 145.12, 155.44, 161.54, 166.13.

## RESULTS AND DISCUSSION

### Synthesis and Characterizations

Synthesis of silicone polymers, having azo side groups, by click chemistry route and their characterization are presented in this article. The design of polymers is planned for their use as liquid crystalline polymers as well as photoactuators. The siloxane backbone is chosen with an idea of allowing a higher degree of freedom so that azo may work both as a chromophore as well as a mesogen.

The synthesis of trisiloxane-diyne, was done through a four-step synthetic procedure as shown in Scheme 1. The overall yield of the monomer trisiloxane-diyne (4) is found to be 77%. The trisiloxane-diol (3) was successfully synthesized in high yield (95%) using platinum catalyzed (Karstedt's catalyst) hydrosilylation reaction at moderate temperature. Various diazide containing azo monomers were prepared by using procedure as shown in Scheme 1. The final azo monomers with different substitutions at the para position are synthesized and purified successfully. All the monomers are characterized by both  $^1\text{H}$  and  $^{13}\text{C}$  NMR spectra.

The hydroxyl peak of  $^1\text{H}$  NMR spectra of siloxane-diol (3) [ $\delta$  2.6] is found to be absent in trisiloxane-diyne (4), thus indicating the completion of the reaction. The other peak positions of trisiloxane-diol (3) are also found to be shifted downfield in trisiloxane-diyne (4). The respective  $^1\text{H}$  NMR peak positions of 10, 11, and 12 also identify the targeted structure.

The polymerizations were carried out by taking equimolar ratio of the trisiloxane-diyne (4) and one of the azo diazides (10–12) in the presence of copper sulfate and sodium ascorbate in an aqueous solution of THF. The reaction was found to be very fast with a completion time of approximately 1 h to obtain a highly viscous polymer solution. The  $^1\text{H}$  NMR spectra shows the appearance of a peak around 7.46–7.48 ppm which can be attributed to the proton in the triazole ring (Fig. 1).

From the GPC results, the molecular weights ( $M_n$ ) of the polymers are found to be in the range of 14,000–35,000  $\text{g mol}^{-1}$ . It can be noted that although the reaction parameters remained same the molecular weight of the polymer varies with the substituents of the azo groups. Polymer P3 has the highest molecular weight whereas polymer P1 has the lowest. All the polymers are soluble in most of the chlorinated solvents and THF. The film-forming properties are also found to be very good.

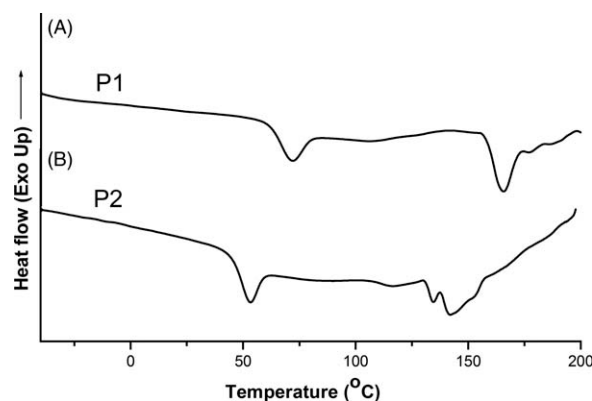


FIGURE 2 DSC Thermogram of polymers P1 (A) and P2 (B).

**TABLE 1** Physico-Chemical Properties of Polymers

Polymer	Thermal Transition (DSC) <sup>a</sup>	POM <sup>b</sup> $T_i$	$M_n$	$M_w$	$M_w/M_n$	$T_d$
P1	C 73 N 165 I	170	14,550	29,200	2.00	210
P2	C 53 S <sub>m</sub> 142 I	149	17,140	40,500	2.36	230
P3	$T_g$ 44	— <sup>c</sup>	33,750	103,600	3.06	275

<sup>a</sup> Transition temperature identified from heating cycle with DSC (at a heating rate of 10°C/min under N<sub>2</sub> atm).

<sup>b</sup> Transition temperature identified with POM at a heating rate of 5°C/min.

<sup>c</sup> Not identified.  $T_d$  = onset degradation temperature of polymers;  $T_i$  = isotropization temperature.

Thermogravimetric analysis (TGA) of the synthesized polymers shows that the polymers possess reasonable stability; only 5% wt loss is observed at 210–275°C. The initial degradation temperature increases from polymer P1 to polymer P3. This may be due to the increase in molecular weight in the order P1 < P2 < P3.

### Liquid Crystalline Property

#### DSC Study

Figure 2 shows the DSC thermogram of polymers P1 and P2 and the data are incorporated in Table 1. It is noted that both the polymers exhibit endothermic peaks; polymer P1

showing two and polymer P2 showing three, respectively. The first one can be attributed to the crystalline (Cr) and liquid crystalline (LC) phase transition. The transition of crystalline phase (Cr) to liquid crystalline phase (LC) for P1 is higher at 73°C whereas for polymer P2 it is 53°C and for P3 the liquid crystallinity is absent. This could be due to the highest ordering/packing efficiency of polymer P1 as the size of the substitution on azo is lowest. In polymer P3, the glass transition temperature is found to be at 44°C. The absence of the LC phase indicates poor ordering of the methyl ester substituent on the azo group. The second endotherm in the DSC thermogram of P1 can be attributed to

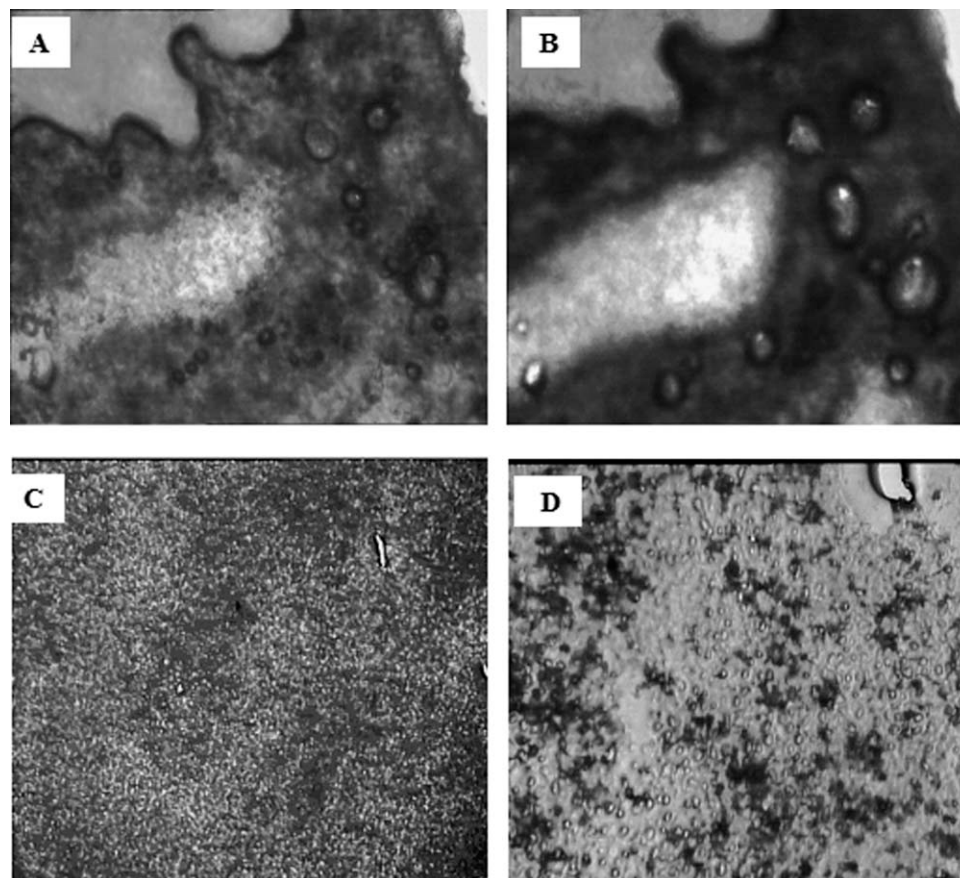


**FIGURE 3** POM images showing nematic droplets texture for P1 at temperature 150°C (A) and 160°C (B) and focal conic texture for P2 at 100°C (C) and threaded type nematic texture at 140°C (D).

**TABLE 2** The Molar Extinction Coefficient of the Diazide Monomers in  $\text{CHCl}_3$ 

Diazide	$\epsilon_{\text{max}}$ ( $\pi - \pi^*$ ) $\text{L mol}^{-1}$ $\text{m}^{-1}$	$\epsilon_{\text{max}}$ ( $n - \pi^*$ ) $\text{L mol}^{-1}$ $\text{cm}^{-1}$
<i>N,N</i> -bis(2-azidoethyl)-4-(phenyldiazenyl) aniline ( <b>10</b> )	21,519	22,456
4-((4-Bis(2-azidoethyl) amino) phenyl) diazenyl) benzonitrile ( <b>11</b> )	24,810	25,783
Methyl 4-((4-(bis(2-azidoethyl) amino) phenyl) diazenyl) benzoate ( <b>12</b> )	32,000	33,594

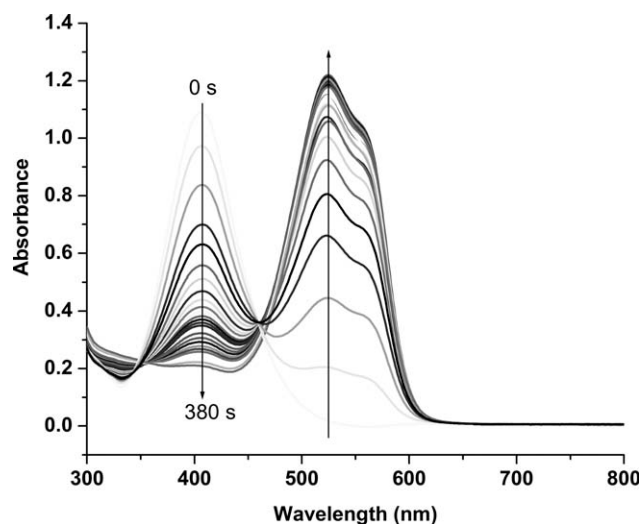
isotropization. For P2, apart from isotropization one more endotherm is observed which appears just before isotropization. This may be due to the appearance of the second LC phase after the first one disappears. The isotropization temperatures of P1 and P2 lie at 165°C and 142°C, respectively.

### POM Study

The mesogenic behaviors were studied by POM. The POM micrographs are shown in Figure 3 and the observation is summarized in Table 1. The appearance of the droplet texture of P1 is observed at 79°C, indicating the presence of nematic phase. At 179°C, the polymer undergoes isotropization. Similarly, polymer P2 exhibits the appearance of a texture characteristic of broken focal conic smectic (SmA) phase [Fig. 3(c)]. A similar texture was also reported by Chao et al. for liquid crystalline polysiloxane containing fluorinated mesogens.<sup>45</sup> On further heating the polymer, the texture changes to droplets type, which is characteristic of nematic state [Fig. 3(d)]. The isotropization temperatures of P1 and P2 are observed to be 170°C and 149°C, respectively. This is near to that observed in the DSC study. Thus, the LC phase extends over a broad temperature range for P1 and P2. The isotropization displays a broad transition for both the polymers P1 and P2. This can be due to the fact that the azo side chain is directly linked through a short spacer to the main chain having siloxane segments in the backbone. In general, broad isotropization temperature is common to side chain liquid crystalline polymers having short spacers.<sup>46</sup>

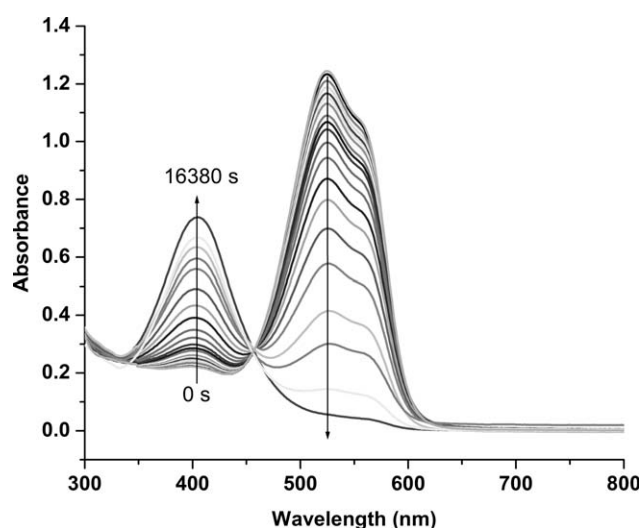
### Photo Responsive Properties

Having azo side groups, the polymers are photoresponsive in nature. The molar extinction coefficient of the diazide monomers (**11–12**) for both  $\pi - \pi^*$  and  $n - \pi^*$  transitions were calculated. During irradiation the diazide monomer shows gradual increase of  $n - \pi^*$  transition peak for *trans-cis* isomerization. The molar extinction coefficient for their  $n - \pi^*$  transition ranges in the order of 22,456 (**10**), 24,810 (**11**), and 33,600 (**12**)  $\text{L mol}^{-1} \text{cm}^{-1}$ , respectively (Table 2). Usually molar extinction coefficient for  $n - \pi^*$  absorption is very low as compared to  $\pi - \pi^*$  absorption. The diazide monomers described here are found to have very high molar extinction coefficient for the  $n - \pi^*$  transition due to the hyperchromic effect of the nitrogen atom attached to the azobenzene group.<sup>43</sup> Due to high intensity absorption for  $n$

**FIGURE 4** UV-Visible absorption spectra in chloroform solution for *trans-cis* isomerization of polymer P3.

$n - \pi^*$  transition in chloroform solution, the color of the solution changes from yellow to orange on UV irradiation indicating rapid transition to *cis* state.

For studying the photoresponsive properties, the chloroform solution of the polymer was kept in dark for three days to assume 100% *trans* form of the azobenzene. Any small amount of *cis* form present is also converted to stable *trans* form. Before irradiation the  $\lambda_{\text{max}}$  absorbance maxima was recorded at 387, 415, and 406 nm for polymers P1, P2, and P3, respectively. This is due to  $\pi - \pi^*$  transition for stable *trans* form. The polymer solutions were then irradiated with UV light (365 nm) for different time intervals and the absorbance vs. wavelength was plotted. Two absorbance peaks are observed in UV-Visible spectra for P3 (Fig. 4). The peaks around 400 and 500 nm can be due to  $\pi - \pi^*$  and  $n - \pi^*$  transitions, respectively. It is found that the absorbance of

**FIGURE 5** UV-Visible absorption spectra in chloroform solution for *cis-trans* isomerization of polymer P3.

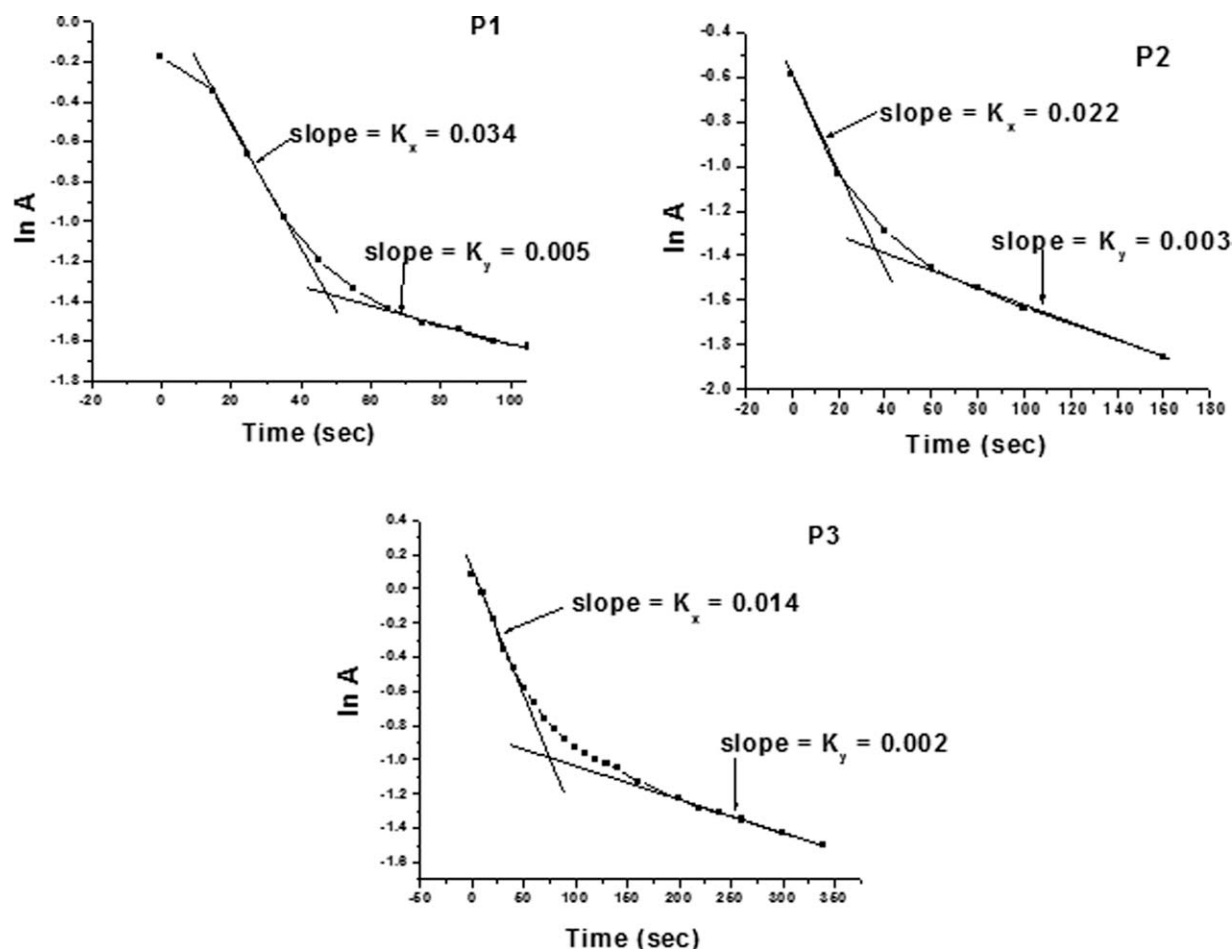


FIGURE 6 Plot of  $\ln A$  vs. time for *trans-cis* isomerization of P1, P2, and P3.

the  $\pi - \pi^*$  electronic transition decreases and  $n - \pi^*$  transition increases with time of irradiation. This phenomenon indicates the conversion of *trans* to *cis* form of the azo polymer. The rate constants of isomerization of the polymers are calculated from slope of the plot of  $\ln A$  vs. time (Fig. 6). All the polymers are found to isomerize within few minutes to the *cis* form. It is observed that shouldering in *cis* peak occurs at a higher wave length during conversion of *trans* to *cis* form. This can be due to solvatochromism; the polar interaction of *cis* azo shifts the absorption spectra to higher wave length.<sup>47</sup> The isomerization process was studied for *cis* to *trans* interconversion for all the three polymers. For this

process, the chloroform solution of polymers was kept under UV irradiation until complete disappearance of  $\pi - \pi^*$  electronic transition as monitored by UV spectra. The samples were then kept in dark and its absorption spectra recorded at different time intervals. It is found that the *cis-trans* isomerization (Fig. 5) of the polymer samples is slow as compared to *trans-cis* photoisomerization (Fig. 4).  $\ln A$  is plotted vs. time for all the polymers. Two slopes ( $K_x$ ,  $K_y$ ) are observed for all the polymers for *trans-cis* isomerization (Fig. 6). The rate constants for *trans-cis* isomerization decrease with increase in molecular weight. It may be due to sluggishness in isomerization. Further, only one slope is

TABLE 3 The Rate Constants of the Polymers for *trans-cis* and *cis-trans* Isomerization

Polymers	$\lambda_{\max}(\text{nm})^a$ $\pi - \pi^*$	$\lambda_{\max}(\text{nm})^a$ $n - \pi^*$	$K_x$ ( $\text{sec}^{-1}$ ) <sup>b</sup>	$K_y$ ( $\text{sec}^{-1}$ ) <sup>c</sup>	$K_z$ ( $\text{min}^{-1}$ ) <sup>d</sup>
P1	387	525	$3.41 \times 10^{-2}$	$5.03 \times 10^{-3}$	$1.18 \times 10^{-4}$
P2	415	525	$2.21 \times 10^{-2}$	$3.80 \times 10^{-3}$	$2.33 \times 10^{-4}$
P3	406	523	$1.41 \times 10^{-2}$	$2.85 \times 10^{-3}$	$4.67 \times 10^{-4}$

<sup>a</sup> Recorded in chloroform solution.

<sup>b</sup> Rate constant calculated from the first slope of *trans* to *cis* isomerization graph ( $\ln A$  vs. time).

<sup>c</sup> Rate constant calculated from the second slope of *trans* to *cis* isomerization graph ( $\ln A$  vs. time).

<sup>d</sup> Rate constant calculated from the slope of *cis* to *trans* isomerization ( $\ln A$  vs. time).

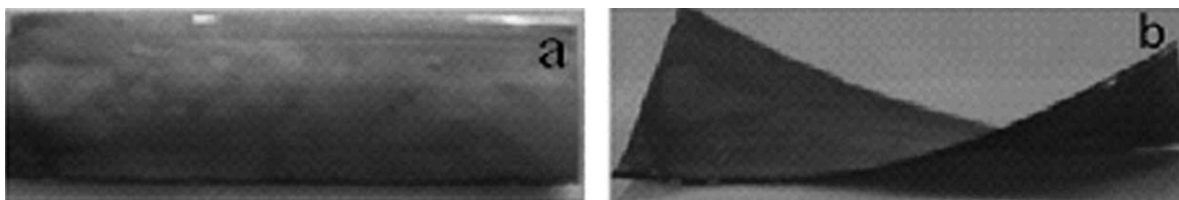


**FIGURE 7** Photomechanical bending of polymer P1 under irradiation with UV light (a) before irradiation (b) after irradiation.

observed for *cis*–*trans* isomerization. This is due to slower process of the latter conversion. Table 3 shows the rate constants for *trans*–*cis* isomerization ( $K_x$ ,  $K_y$ ) and *cis*–*trans* isomerization ( $K_z$ ).

### Photomechanical Properties

For photomechanical study, the free standing film was prepared as a bilayer. Polyvinyl alcohol (PVA) was first cast on a glass slide and rubbed with silk cloth in one direction. The azo polymer solution in THF was later cast on the PVA film to make a bilayer. The bilayer was made as the azo polymer free standing film which was very fragile.

The photoactuation of the polymers was studied by irradiation with 365-nm irradiation. The PVA-Azo polymer P1 was subjected to irradiation for its photomechanical effect. The onset of bending of PVA-Azo bilayer is observed during a typical irradiation intensity of 5500–6500  $\mu\text{W}/\text{cm}^2$ . The bending increases as the isomerization of *trans*–*cis* azo goes further. After 15 min, the bending angle is observed around 45° (Fig. 7). The bent film on being kept in the dark for a long period of time regains the original shape, indicating the transformation from *cis* to *trans* form.

### CONCLUSIONS

Three types of siloxane polymers possessing both photoactive and liquid crystalline properties have been successfully prepared using click chemistry route. The polymers P1 and P2 showed liquid crystalline characteristics existing at a broad temperature range and all the three polymers showed photoactive properties. The rate constants for *trans*–*cis* isomerization decreases with an increase in the molecular weight of the polymers. The rate of *trans*–*cis* isomerization was found to be higher than that of *cis*–*trans* isomerization. The *trans*–*cis* isomerization has led to bending of bilayer film, thus showing photomechanical effect.

### REFERENCES AND NOTES

- Hartley, G. S. *Nature* **1937**, *140*, 281.
- Rau, H. In *Photochemistry and Photophysics*; Rebek, J. F., Ed.; CRC Press: Boca Raton, FL, **1990**; Vol. 2, pp 119–141.
- Natansohn, A.; Rochon, P. *Chem. Rev.* **2002**, *102*, 4139–4175.
- Yu, Y.; Nakano, M.; Ikeda, T. *Nature* **2003**, *425*, 145.
- (a) Imrie, C. T.; Karasz, F. E.; Attard, G. S. *Macromolecules* **1993**, *26*, 545–550; (b) Lee, J. H.; Lee, K. S. *Bull. Korean Chem. Soc.* **2000**, *21*, 847–848; (c) Izumi, A.; Teraguchim, M.; Nomura, R.; Masuda, T. *J. Polym. Sci. Part A: Polym. Chem.* **2000**, *38*, 1057–1063; (d) Castell, P.; Galia, M.; Serra, A. *Macromol. Chem. Phys.* **2001**, *202*, 1649–1657; (e) Turkey, G.; Schonhals, A. *Polymer* **2004**, *45*, 255–262; (f) Wang, H.; He, Y.; Tuo, X.; Wang, X. *Macromolecules* **2004**, *37*, 135–146.
- Alazaroaie, S.; Toader, V.; Carlescu, I.; Kazmierski, K.; Scutaru, D.; Hurduc, N.; Simionescu, I. *Eur. Polym. J.* **2003**, *39*, 1333–1339.
- McArdle, C. B. In *Side Chain Liquid Crystal Polymers*; McArdle, C. B., Ed.; Blackie and Sons: Glasgow, **1989**; Chapter 13.
- Percec, V.; Tomazos, D. *Adv. Mater.* **1992**, *4*, 548–561.
- Donald, A. M.; Windle, A. H.; Hanna, S. In *Liquid Crystalline Polymers*; Cambridge University Press: Cambridge, UK, **2006**; Part 1, pp. 8.
- Kwon, Y. K.; Chvalun, S. N.; Blackwell, J.; Percec, V.; Heck, J. A. *Macromolecules* **1996**, *28*, 1552–1558.
- Rudick, J. G.; Percec, V. *Acc. Chem. Res.* **2008**, *41*, 1641–1652.
- Percec, V.; Schlueter, D.; Kwon, Y. K.; Blackwell, J. *Macromolecules* **1996**, *28*, 8807–8818.
- Percec, V.; Rudick, J. G.; Peterca, M.; Martin Wagner, M.; Obata, M.; Mitchell, C. M.; Cho, W.-D.; Venkatachalapathy, B. S. K.; Heiney, P. A. *J. Am. Chem. Soc.* **2005**, *127*, 15257–15264.
- Rosen, B. M.; Wilson, C. J.; Wilson, D. A.; Peterca, M.; Imam, M. R.; Percec, V. *Chem. Rev.* **2009**, *109*, 6275–6540.
- Percec, V.; Dulcey, A. E.; Venkatachalapathy, B. S. K.; Miura, Y.; Smidrkal, J.; Peterca, M.; Nummelin, S.; Edlund, U.; Hudson, S. D.; Heiney, P. A.; Hu Duan, H.; Magonov, S. N.; Vinogradov, S. A. *Nature* **2004**, *430*, 764–768.
- Percec, V.; Glodde, M.; Bera, T. K.; Miura, Y.; Shiyanovskaya, I.; Singer, K. D.; Balagurusamy, V. S. K.; Heiney, P. A.; Schnell, I.; Rapp, A.; Spiess, H. W.; Hudson, S. D.; Duan, H. *Nature* **2002**, *417*, 384–387.
- Angeloni, A. S.; Carretti, D.; Carlini, C.; Chiellini, E.; Altomare, A.; Solaro, R.; Laus, M. *Liquid Crystals*, **1989**, *4*, 513–527.
- Percec, V.; Ahn, C. H.; Ungar, G.; Yearley, D. J. P.; Möller, M.; Sheiko, S. S. *Nature* **1998**, *391*, 161–164.
- Percec, V.; Johansson, G.; Ungar, G.; Zhou, J. *J. Am. Chem. Soc.* **1996**, *118*, 9855–9866.
- Percec, V.; Ahn, C.-H.; Cho, W.-D.; Jamieson, A. M.; Kim, J.; Leman, T.; Schmidt, M.; Gerle, M. M.; Prokhorova, S. A.; Sheiko, S. S.; Cheng, S. Z. D.; Zhang, A.; Ungar, G.; Yearley, D. J. P. *J. Am. Chem. Soc.* **1998**, *120*, 8619–8631.
- Percec, V.; Kawasumi, M. *Macromolecules* **1992**, *25*, 3843–3850.
- Percec, V.; Chu, P.; Kawasumi, M. *Macromolecules* **1994**, *27*, 4441–4453.
- Percec, V.; Chu, P.; Ungar, G.; Zhod, J. *J. Am. Chem. Soc.* **1995**, *117*, 11441–11454.
- Percec, V.; Lee, M. *Macromolecules* **1991**, *24*, 2780–2788.
- Percec, V.; Heck, J. A.; Tomazos, D.; Ungar, G. *J. Chem. Soc. Perkin Trans.* **1993**, *2*, 2381–2388.
- Percec, V.; Tomazos, D.; Pugh, C. *Macromolecules*, **1989**, *22*, 3259–3267.

- 27** Yager, K. G.; Barrett, C. J. *Macromolecules*, **2006**, *39*, 9320–9326.
- 28** (a) de Gennes P. G. *Phys. Lett. A*, **1969**, *28*, 725–726; (b) Verploegen, E.; Soulages, J.; Kozberg, M.; Zhang, T.; McKinley, G.; Hammond, P. *Angew Chem. Int. Ed.* **2009**, *48*, 3494–3498.
- 29** (a) Ikeda, T.; Mamiya, J.-I.; Yu, Y. L. *Angew Chem.* **2007**, *119*, 512–535; *Angew Chem. Int. Ed.* **2007**, *46*, 506–528; (b) Hrozhyk, U. A.; Serak, S. V.; Tabiryan, N. V.; Bunning, T. J. *J. Adv. Mater.* **2007**, *19*, 3244–3247.
- 30** Kumar, S. *Chem. Rev.* **1989**, *89*, 1915–1925.
- 31** Hogan, P. M.; Tajbakhsh, A. R.; Terentjev, E. M. *Phys. Rev. E* **2002**, *65*, 041720–041729.
- 32** Kim, N.; Li, Q.; Kyu, T. *Phys. Rev. E* **2011**, *83*, 031702–031709.
- 33** Shioji, Y.; Ishige, R.; Higashihara, T.; Watanabe, J.; Ueda, M. *Macromolecules* **2010**, *43*, 805–810.
- 34** (a) Finkelmann, H.; Rehage, G. *Makromol. Chem. Rapid Commun.* **1980**, *1*, 733–740; (b) Finkelmann, H. *Macromol. Chem.* **1982**, *183*, 1245–1256.
- 35** Rousseau I. A.; Qin, H.; Mather, P. T. *Macromolecules* **2005**, *38*, 4103–4113.
- 36** Percec, V.; Heck, J.; Ungar, J. *Macromolecules* **1991**, *24*, 4957–4962.
- 37** (a) Percec, V.; Tomazos, D. *Macromolecules* **1989**, *22*, 2062–2069; (b) Percec, V.; Tomazos, D. *Macromolecules* **1989**, *22*, 1512–1514.
- 38** Percec, V.; Rodenhouse, R. *Macromolecules* **1989**, *22*, 4408–4412.
- 39** Hahn, B.; Percec, V. *Macromolecules*, **1987**, *20*, 1588–1599.
- 40** (a) Percec, V.; Hahn, B. *Macromolecules* **1989**, *22*, 1588–1599; (b) Percec, V.; Hahn, B.; Ebert, M.; Wendorff, J. H. *Macromolecules* **1990**, *23*, 2092–2095.
- 41** Racles, C.; Airinei, A.; Cozan, V.; Cazacu, M.; Sajo I. E. *J. Appl. Polym. Sci.*, **2003**, *90*, 3093–3099.
- 42** (a) Li, Z.; Yu, G.; Hu, P.; Ye, C.; Liu, Y.; Qin, J.; Li, Z. *Macromolecules* **2009**, *42*, 1589–1596; (b) Li, Z.; Wu, W.; Qiu, G.; Liu, Y.; Ye, C.; Qin, J.; Li, Z. *J. Polym. Sci. Part A: Polym. Chem.*, **2011**, *49*, 1977–1987; (c) Qin, A.; Lam, J. W. Y.; Tang, L.; Jim, C. K. W.; Zhao, H.; Sun, J.; Tang, B. Z. *Macromolecules* **2009**, *42*, 1421–1424; (d) Meudtner, R.; Hecht, S.; *Macromol. Rapid Commun.* **2008**, *29*, 347–351; (e) Nagao, Y.; Takasu, A. *Macromol. Rapid Commun.* **2009**, *30*, 199–203; (f) Binauld, S.; Damiron, D.; Hamaide, T.; Pascault, J.-P.; Fleury, E.; Drokenmuller, E. *Chem. Commun.* **2008**, *35*, 4138–4140; (g) Chernykh, A.; Agag, T.; Ishida, H. *Polymer* **2009**, *50*, 382–390.
- 43** Metha, R.; Paradorn, N.; Pranee, P. *Polymer* **2005**, *46*, 9742–9752.
- 44** Shen, X.; Liu, H.; Li, Y.; Liu, S. *Macromolecules* **2008**, *41*, 2421.
- 45** Zhu, X.; Beginn, U.; Moller, M.; Gearba, R.; Anokhin, D.; Ivanov, A. *J. Appl. Polym. Sci.* **2006**, *128*, 16928–16937.
- 46** Meng, F.-B.; Cui, Y.; Chen, H.-B.; Zhang, B.-Y.; Jia, C. *Polymer* **2009**, *50*, 1187–1196.
- 47** Freiberg, S.; Labarthe, F. L.; Rochon, P.; Natansohn, A. *Macromolecules* **2003**, *36*, 2680–2688.